An Experimental Study of Rich Premixed Gasoline/O 2 /Ar Flame with Tunable Synchrotron Vacuum Ultraviolet Photoionization

ARTICLE *in* ENERGY & FUELS · JULY 2007

Impact Factor: 2.79 · DOI: 10.1021/ef0700578

An Experimental Study of Rich Premixed Gasoline/O_2/Ar Flame with Tunable Synchrotron Vacuum Ultraviolet Photoionization

Yuyang Li, Chaoqun Huang, Lixia Wei, Bin Yang, Jing Wang, Zhenyu Tian, Taichang Zhang, Liusi Sheng, and Fei Qi*

National Synchrotron Radiation Laboratory, University of Science and Technology of China, Hefei, Anhui 230029, P. R. China

Received January 29, 2007. Revised Manuscript Received May 7, 2007

In this work, a rich premixed gasoline/O_2/Ar flame at low pressure (30 Torr) with an equivalence ratio (ϕ) of 1.73 is investigated and reported. The identification and mole fraction calculation of most flame species, including isomeric intermediates, are performed in this study using the tunable synchrotron photoionization and molecular-beam mass spectrometry techniques, and the flame temperature profile is recorded using a Pt/Pt-13%Rh thermocouple. The possible formation pathways of some flame species, such as 1,3-butadiene, benzene, and naphthalene, are discussed in this paper, along with the comparison between this flame and other premixed hydrocarbon flames. It is concluded that the mole fraction of 1,3-butadiene is strongly related to that of the 1-buten-3-yl radical in the hydrocarbon flames. The decomposition of higher aromatics is found to be more important for benzene formation in this flame than the recombination of small intermediates, while the intermediate reactions are suggested as the dominant formation pathway of naphthalene. The comprehensive experimental data will be helpful for understanding the combustion mechanism of gasoline and pursuing a better control of exhaust emission levels from gasoline-fueled engines.

1. Introduction

Gasoline is the major distillation product of petroleum, consisting of paraffins, olefins, and aromatics with 5 to 12 carbon atoms.[1] Its combustion in Otto (spark-ignited) engines can provide power to vehicles and machines, which has greatly promoted the development of human society and the world economy in the past century. However, the exhaust emissions from gasoline-fueled engines such as hydrocarbons, oxygenated organic compounds, carbon monoxide, and nitrogen oxides (NO_x) can cause a lot of environmental problems, especially in some urban areas. Many investigations indicated that some emissions are toxic to the human body. For example, 1,3-butadiene, benzene, toluene, ethylbenzene, xylene, and polycyclic aromatic hydrocarbons (PAHs) are considered to be mutagenic or carcinogenic, while formaldehyde and most other aldehydes may contribute to the formation of photochemical smog or cause irritation of the skin, eyes, and nasopharyngeal membranes.[2−5] It has been proven that the chemical composition and magnitude of exhaust emissions varies with the gasoline composition.[6] Thus, continuing efforts based on this strategy, for example, reformulating the gasoline composition, have been made to reduce hazardous emissions.

Since the middle of the past century, the public's growing concern for better air quality and the strict legislation enacted by many countries to limit vehicle exhaust emissions have attracted researchers to study gasoline combustion in laboratory burners and real engines. The problem is that gasoline is an extremely complex mixture containing hundreds of organic compounds, which makes its combustion mechanism hard to be clearly understood. Hence, most previous research in this field focused on the detection of exhaust emission levels and combustion characteristics via several techniques, for example, Fourier-transform infrared spectroscopy,[5] gas chromatography (GC),[7] mass spectrometry (MS) with chemical ionization, selected ion flow tube and atmospheric pressure ionization methods,[8−11] and GC combined with MS (GC/MS).[3,12,13] These works have enormously extended our knowledge about how to increase combustion efficiency and reduce exhaust emissions of gasoline-fueled engines. However, a detailed combustion mechanism of gasoline is still beyond our sight because combustion intermediates in these works were insufficiently identified, and the development of new online methods which can achieve a sensitive and selective detection of intermediates and exhaust species is needed.[6,14]

* Corresponding author. Tel.: 86-551-3602125. Fax: 86-551-5141078. E-mail: fqi@ustc.edu.cn.

(1) Wang, J.; Yang, B.; Li, Y. Y.; Tian, Z. Y.; Zhang, T. C.; Qi, F. *Int. J. Mass Spectrom.* **2007**, *263*, 30−37.
(2) Koshland, C. P. *Proc. Combust. Inst.* **1996**, *26*, 2049−2065.
(3) Marr, L. C.; Kirchstetter, T. W.; Harley, R. A.; Miguel, A. H.; Hering, S. V.; Hammond, S. K. *Environ. Sci. Technol.* **1999**, *33*, 3091−3099.
(4) Mitchell, C. E.; Olsen, D. B. *J. Eng. Gas Turbines Power* **2000**, *122*, 603−610.
(5) Al-Farayedhi, A. A. *Int. J. Energy Res.* **2002**, *26*, 279−289.
(6) Schuetzle, D.; Siegl, W. O.; Jensen, T. E.; Dearth, M. A.; Kaiser, E. W.; Gorse, R.; Kreucher, W.; Kulik, E. *Environ. Health Perspect.* **1994**, *102* (Suppl.), 3−12.
(7) Zervas, E.; Montagne, X.; Lahaye, J. *Environ. Sci. Technol.* **2002**, *36*, 2414−2421.
(8) Dearth, M. A.; Glerczak, C. A.; Siegl, W. O. *Environ. Sci. Technol.* **1992**, *26*, 1573−1580.
(9) Heeb, N. V.; Forss, A. M.; Bach, C.; Reimann, S.; Herzog, A.; Jackle, H. W. *Atmos. Environ.* **2000**, *34*, 3103−3116.
(10) Smith, D.; Cheng, P.; Spanel, P. *Rapid Commun. Mass Spectrom.* **2002**, *16*, 1124−1134.
(11) Heeb, N. V.; Forss, A. M.; Saxer, C. J.; Wilhelm, P. *Atmos. Environ.* **2003**, *37*, 5185−5195.
(12) Hakansson, A.; Stromberg, K.; Pedersen, J.; Olsson, J. O. *Chemosphere* **2001**, *44*, 1243−1252.
(13) Riservato, M.; Rolla, A.; Davoli, E. *Rapid Commun. Mass Spectrom.* **2004**, *18*, 399−404.
(14) Butcher, D. J. *Mirochem. J.* **2000**, *66*, 55−72.

10.1021/ef0700578 CCC: $37.00
Published on Web 06/22/2007

In the past decade, mass spectrometry combined with the vacuum ultraviolet (VUV) single-photon ionization (SPI) or resonance-enhanced multiphoton ionization (REMPI) techniques has been developed for the research of gasoline combustion.[15−17] SPI and REMPI have been proven to be soft ionization methods, which can minimize the interference from fragment ions and realize the selective detection of flame species. More recently, a new SPI method that employs synchrotron radiation as an ionization source has been developed in combination with the molecular-beam mass spectrometry (MBMS) technique.[18−20] Compared with those laser-employed SPI methods, this new method can detect more flame species due to the tunability of synchrotron light in the VUV region.

Generally speaking, the combustion processes in Otto engines can be approximated as premixed flames started by spark ignition. However, few premixed gasoline flames have been studied before. Using the GC/MS method, Hakansson et al. investigated the combustion of gasoline ($\phi = 1 \pm 0.1$) with two different qualities.[12] They detected about 40 compounds and discussed the differences between emissions from the two flames. Unfortunately, their work contains no active flame species like radicals and unstable combustion intermediates, due to the limitations of GC/MS. A recent study by Huang et al. revealed the detailed chemical structure of a lean gasoline flame ($\phi = 0.75$).[21] About 80 flame species were observed, including a large amount of flame intermediates. However, to the best of our knowledge, no investigation has been performed on the rich premixed gasoline flame.

Here, we present a premixed gasoline/O_2/Ar flame with an equivalence ratio of 1.73 at low pressures. The synchrotron VUV photoionization and MBMS techniques are utilized to detect flame species in this work. Due to the high resolution of photoionization mass spectrometry and tunable photon energy in the VUV region, most flame species, for example, hydrocarbons, radicals, and oxygenated compounds, are clearly observed and identified. Isomeric intermediates are unambiguously distinguished, which can help us to get a better insight of the chemistry in gasoline flames. Meanwhile, mole fraction profiles of observed intermediates are calculated, which can satisfy the further needs of modeling studies.

2. Experimental Section

2.1. Instrument. The experimental work was performed at the flame endstation of the National Synchrotron Radiation Laboratory in Hefei, China. The instrument has been reported elsewhere.[20,22,23] Briefly, it consists of a low-pressure flame chamber, a differentially pumped chamber with a molecular-beam sampling system, and a photoionization chamber with a reflectron time-of-flight mass spectrometer (RTOF-MS).[24] In the flame chamber, there is a 6.0-cm-diameter McKenna burner with a laminar flat flame stabilized on the surface. A quartz conelike nozzle with a 40° included angle and a ~500 μm orifice at the tip is used to sample the flame species. The sampled gas forms a molecular beam which then passes into a differentially pumped ionization region through a nickel skimmer. The molecular beam is crossed by the tunable synchrotron light between the repeller and extractor plates of the RTOF-MS. Molecules with ionization energies (IEs) lower than the photon energy will be ionized; then, the produced photoions are collected and analyzed by the RTOF-MS, which has an approximate mass resolving power ($m/\Delta m$) of 1400. The synchrotron radiation from a bending magnet beamline of the 800 MeV electron storage ring is dispersed by a 1 m Seya-Namioka monochromator equipped with a 1200 grooves/mm grating. The energy resolution ($E/\Delta E$) is about 500 with ~150 μm entrance and exit slits. A LiF window of 1.0 mm thickness is mounted between the exit slit and the photoionization chamber to eliminate higher-order harmonic radiation when the wavelength is longer than 105 nm.

Table 1. Gasoline Specifications

density (kg·L^{-1})	0.737
10 vol % evaporated boiling point (°C)	59
50 vol % evaporated boiling point (°C)	105
90 vol % evaporated boiling point (°C)	159
final boiling point (°C)	184
Compositions (vol %)	
paraffins	47
olefins	29
aromatics	24

2.2. Experimental Conditions. The 90# standard unblended gasoline for this experiment was produced by Fangyuan Inc., China. The specifications of the gasoline are also measured by the vendor, as listed in Table 1. A syringe pump (ISCO 1000D, USA) was used to inject gasoline into the vaporizer (473 K) with a liquid flow rate of 1.400 mL/min at room temperature. The gas flow rates of O_2 and Ar were 1.400 and 1.000 standard liters per minute (SLM), which were controlled separately by MKS mass flow controllers. In this work, the pressure in the flame chamber is maintained at 30 Torr (4.00 kPa) to stabilize the flame. Thus, the inlet cold-flow (300 K) velocity is 39.07 cm/sec, and the mass flow rate of the reagent is 2.840×10^{-3} g/sec·cm^2. The experimental conditions were chosen to get a stable rich premixed flame at low pressures.

In general, the equivalence ratio of a gasoline flame is hard to determine due to the complex composition of gasoline. Previous studies usually treated gasoline as a C_7 or C_8 aliphatic hydrocarbon. For example, Hakansson et al. approximated their gasolines as a C_7 alkene,[12] while Huang et al. used isooctane to calculate the equivalence ratio.[21] Recently, we analyzed the composition of the gasoline used for this experiment with the synchrotron VUV photoionization technique.[1] On the basis of the comprehensive species identification and concentration measurement, we simplified the gasoline to be a hydrocarbon with a molecular formula of C_mH_n and calculated the respective values of m and n to be 7.74 and 13.88. Therefore, the equivalence ratio is derived to be 1.73 ± 0.01 for this gasoline flame.

The temperature profile was measured using a Pt/Pt-13%Rh thermocouple, 0.076 mm in diameter and 15 mm upstream from the sampling nozzle and coated with Y_2O_3−BeO anticatalytic ceramics to avoid catalytic effects.[25] Radiative heat losses, as well as the perturbations caused by the thermocouple, were considered and calibrated for the temperature profile.[26] The experimental error is estimated to be ±100 K. For further studies of modeling, the

(15) Butcher, D. J. *Mirochem. J.* **1999**, *62*, 354−362.
(16) Butcher, D. J.; Goeringer, D. E.; Hurst, G. B. *Anal. Chem.* **1999**, *71*, 489−496.
(17) Zimmermann, R. *Anal. Bioanal. Chem.* **2005**, *381*, 57−60.
(18) Cool, T. A.; Nakajima, K.; Mostefaoui, T. A.; Qi, F.; McIlroy, A.; Westmoreland, P. R.; Law, M. E.; Poisson, L.; Peterka, D. S.; Ahmed, M. *J. Chem. Phys.* **2003**, *119*, 8356−8365.
(19) Cool, T. A.; McIlroy, A.; Qi, F.; Westmoreland, P. R.; Poisson, L.; Peterka, D. S.; Ahmed, M. *Rev. Sci. Instrum.* **2005**, *76*, 094102.
(20) Qi, F.; Yang, R.; Yang, B.; Huang, C. Q.; Wei, L. X.; Wang, J.; Sheng, L. S.; Zhang, Y. W. *Rev. Sci. Instrum.* **2006**, *77*, 084101.
(21) Huang, C. Q.; Wei, L. X.; Yang, B.; Wang, J.; Li, Y. Y.; Sheng, L. S.; Zhang, Y. W.; Qi, F. *Energy Fuels* **2006**, *20*, 1505−1513.
(22) Yang, B.; Li, Y. Y.; Wei, L. X.; Huang, C. Q.; Wang, J.; Tian, Z. Y.; Yang, R.; Sheng, L. S.; Zhang, Y. W.; Qi, F. *Proc. Combust. Inst.* **2007**, *31*, 555−563.
(23) Yang, B.; Osswald, P.; Li, Y. Y.; Wang, J.; Wei, L. X.; Tian, Z. Y.; Qi, F.; Kohse-Hoinghaus, K. *Combust. Flame* **2007**, *148*, 198−209.
(24) Huang, C. Q.; Yang, B.; Yang, R.; Wang, J.; Wei, L. X.; Shan, X. B.; Sheng, L. S.; Zhang, Y. W.; Qi, F. *Rev. Sci. Instrum.* **2005**, *76*, 126108.
(25) Kent, J. H. *Combust. Flame* **1970**, *14*, 279−281.
(26) Fristrom, R. M. *Flame Structure and Processes*; Oxford: New York, 1995; p 118−119; p 175.

temperature profile should be lowered by 100 K to account approximately for the cooling effect of the sampling probe.[27,28]

2.3. Procedures. With the variation of photon energy, a series of mass spectra can be taken at the specified burner position (usually in the middle of the visible flame region) for measurement of the photoionization efficiency (PIE) spectra. The integrated ion intensities for a specific mass are normalized by the photon flux recorded by a silicon photodiode and plotted as a function of the photon energy, which then yields the PIE spectra containing precise IE information of the corresponding species. This method has been used for identifying combustion intermediates successfully.[18−23] When the energy resolution of the monochromator and the cooling effect of molecular beam are considered,[29] the experimental errors for measured IEs are 0.05 eV for species with strong signals and 0.10 eV for species with weak signals.

Movement of the burner toward or away from the quartz nozzle allows a mass spectrum to be taken at an arbitrary position in the flame. In order to keep near-threshold ionization and avoid fragmentation, we scan the burner position at selected photon energies. The mole fractions of flame species can be derived according to the method described by Cool et al.[30] However, a problem for mole fraction calculation in this work must be noticed, that the fuel is a mixture of hydrocarbons and it is hard for us to directly use this method which deduces the mole fractions of combustion intermediates from that of the fuel. To solve this problem, a small quantity of acetylene was added to the flame for calibration; the flow rate of additive acetylene was changed (0.02, 0.03, 0.04, and 0.05 SLM) in order to measure the relationship between its signal and initial mole fraction, from which the mole fraction of acetylene near the burner surface in the undoped flame could be deduced. On the basis of the known spatial profile of acetylene's signal, we can get its mole fraction profile in this flame. Finally, mole fractions of other intermediates can be calculated from that of acetylene. In addition, the calculation needs photoionization cross sections, which are available for most small flame species with molecular weights less than 78.[18,31−35] For those intermediates with unknown photoionization cross sections, a method reported by Koizumi is used to estimate the cross section value.[36] In this work, no correction has been made for the mole fraction profiles to compensate for the fact that the sampling cone draws from a flame region extending several nozzle diameters ahead of the cone.[26,37] The mole fractions should have an uncertainty of ±25% for stable molecules and a factor of 2 for radicals and intermediates with estimated cross sections.

3. Results

3.1. Photoionization Mass Spectrum. Figure 1 presents a photoionization mass spectrum of the rich gasoline flame, taken at a photon energy of 11.81 eV and a burner position of 6.5 mm, which is inside the luminous zone of the flame. As shown in the figure, relative ion signals are amplified with factors of 5, 30, and 50 for different mass regions to clearly reveal the weak peaks. A lot of mass peaks can be observed from the mass spectrum, each corresponding to one or more species which may be combustion intermediates or fragment ions from photoionization. In fact, the appearance potentials (APs) of most fragment ions are higher than the IEs of intermediates with the same or close molecular weight. Thus, the interference of fragment ions can be avoided if the photon energy is selected between the IEs of intermediates and APs of fragment ions.

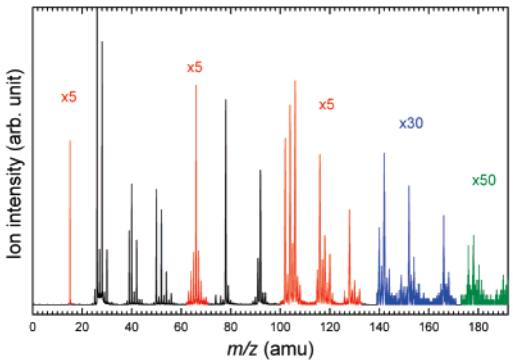

Figure 1. Photoionization mass spectrum of the rich gasoline flame, taken at a burner position of 6.5 mm and a photon energy of 11.81 eV. Partial ion signals are amplified with factors of 5, 30, and 50 for different mass regions as shown in the figure.

The other interference is from the isomers. The total number of possible isomers increases rapidly with the number of atoms, and they always play different roles in combustion processes because of their different structural features and chemical properties. Hence, isomeric identification is crucial for understanding the flame chemistry. Measurement of PIE spectra of each observed mass can provide information on ionization thresholds, which can help us distinguish isomeric intermediates unambiguously. In this work, most flame species, including hydrocarbons, oxygenated hydrocarbons, and radicals, are identified and listed in Table 2, along with their measured IEs, peak positions, and maximum mole fractions. The identification of combustion intermediates will be illustrated in detail with several representative PIE spectra as follows.

3.2. Photoionization Efficiency Spectra. Figures 2−4 illustrate species identification in this flame, with the recommended species and their literature IEs marked above the observed thresholds. All PIE spectra were measured at 6.5 mm. The combustion intermediates can be classified as four types, that is, small hydrocarbons with a molecular weight less than 78 serving as intermediates for the oxidation of fuels and formation of large hydrocarbons, oxygenated hydrocarbons, radicals, and large hydrocarbons (most of which are aromatic species).

Figure 2 shows four PIE spectra of small hydrocarbon intermediates with a molecular weight less than 70 in this flame. As seen in Figure 2a, two clear thresholds at 9.74 and 10.35 eV can be attributed to the photoionization of allene (IE = 9.69 eV)[38] and propyne (IE = 10.36 eV).[38] No other obvious onset can be observed on the PIE spectra, indicating that allene and propyne contribute mostly to the ion signals of $m/z = 40$. Figure 2b shows the PIE spectra of $m/z = 52$ with photon energies ranging from 8.00 to 10.50 eV. The threshold near 9.56 eV implies that the dominant species of this mass is vinylacetylene, which has a literature IE of 9.58 eV.[38] The spectra between photon energies of 8.72 and 9.29 eV are amplified by a factor

(27) Biordi, J. C.; Lazzara, C. P.; Papp, J. F. *Combust. Flame* **1974**, *23*, 73−82.
(28) Stepowski, D.; Puechberty, D.; Cottereau, M. J. *Proc. Combust. Inst.* **1981**, *18*, 1567−1573.
(29) Kamphus, M.; Liu, N. N.; Atakan, B.; Qi, F.; McIlroy, A. *Proc. Combust. Inst.* **2002**, *29*, 2627−2633.
(30) Cool, T. A.; Nakajima, K.; Taatjes, C. A.; McIlroy, A.; Westmoreland, P. R.; Law, M. E.; Morel, A. *Proc. Combust. Inst.* **2005**, *30*, 1681−1688.
(31) Person, J. C.; Nicole, P. P. *J. Chem. Phys.* **1968**, *49*, 5421−5426.
(32) Person, J. C.; Nicole, P. P. *J. Chem. Phys.* **1970**, *53*, 1767−1774.
(33) Robinson, J. C.; Sveum, N. E.; Neumark, D. M. *J. Chem. Phys.* **2003**, *119*, 5311−5314.
(34) Robinson, J. C.; Sveum, N. E.; Neumark, D. M. *Chem. Phys. Lett.* **2004**, *383*, 601−605.
(35) Cool, T. A.; Wang, J.; Nakajima, K.; Taatjes, C. A.; McIlroy, A. *Int. J. Mass Spectrom.* **2005**, *247*, 18−27.
(36) Koizumi, H. *J. Chem. Phys.* **1991**, *95*, 5846−5852.
(37) Hartlieb, A. T.; Atakan, B.; Kohse-Hoinghaus, K. *Combust. Flame* **2000**, *121*, 610−624.
(38) Linstrom, P. J.; Mallard, W. G. *NIST Chemistry Webbook*; National Institute of Standards and Technology: Gaithersburg, MD, 2005.

Table 2. List of Combustion Intermediates Measured in the Rich Gasoline Flame, along with Their IEs, Peak Positions, and Maximum Mole Fractions (X_{MAX})

			IE (eV)		mole fraction	
mass	formula	species	literature[a]	measured[b]	peak position (mm)	X_{MAX}
15	CH_3	methyl radical	9.84	9.80	7.0	3.61E-03
26	C_2H_2	acetylene	11.40	11.37	8.0	2.00E-02
27	C_2H_3	vinyl radical	8.59	8.66	8.0	2.52E-05
28	C_2H_4	ethylene	10.51	10.51	6.5	1.24E-02
29	C_2H_5	ethyl radical	8.26	8.32	6.0	4.07E-04
30	H_2CO	formaldehyde	10.88	10.85	5.0	2.46E-03
32	CH_3OH	methanol	10.85	10.83	4.0	1.67E-04
39	C_3H_3	propargyl radical	8.67	8.69	8.0	3.10E-03
40	C_3H_4	allene	9.69	9.74	7.5	6.36E-04
		propyne	10.36	10.35	7.0	1.34E-03
41	C_3H_5	allyl radical	8.14	8.14	6.0	1.39E-03
42	C_2H_2O	ketene	9.62	9.61	6.5	2.45E-03
	C_3H_6	propylene	9.73	9.72	6.5	4.76E-03
43	C_3H_7	isopropyl radical	7.37	7.42	7.0	2.86E-05
44	C_2H_4O	ethenol	9.33	9.32	6.5	6.92E-05
		acetaldehyde	10.23	10.25	6.0	1.63E-04
50	C_4H_2	diacetylene	10.17	10.16	8.5	2.28E-03
51	C_4H_3	CH_2CCCH (i-C_4H_3)	8.02[c]	8.01	8.0	2.21E-05
52	C_4H_4	1,2,3-butatriene	9.15	9.15	7.5	1.20E-04
		vinylacetylene	9.58	9.56	7.5	1.38E-03
53	C_4H_5	but-2-yn-1-yl radical	7.95[c]	7.95	7.5	3.75E-05[d]
		1-butyn-3-yl radical	7.97[c]			
		CH_2CHCCH_2 (i-C_4H_5)	7.60[c]	7.57	7.5	6.26E-06
54	C_4H_6	1,3-butadiene	9.07	9.07	6.5	5.76E-03
55	C_4H_7	1-buten-3-yl radical	7.49	7.54	6.5	1.44E-04
56	C_3H_4O	methylketene	8.95	8.94	3.0	1.19E-04
	C_4H_8	2-butene	9.11	9.13	6.5	1.64E-03
63	C_5H_3	HCCCHCCH (n-C5H3)	8.32[e]	8.32	7.0	1.21E-04
64	C_5H_4	1,2,3,4-pentatetraene	8.67	8.65		trace level
		1,3-pentadiyne	9.50	9.50	8.0	2.25E-04
65	C_5H_5	cyclopentadienyl radical	8.41	8.45	6.5	6.42E-04
66	C_5H_6	1,3-cyclopentadiene	8.57	8.57	6.0	2.98E-03
68	C_5H_8	1,3-pentadiene	8.62	8.61	6.5	1.58E-03
		2-methyl-1,3-butadiene	8.86	8.85	6.5	6.33E-04
74	C_6H_2	1,3,5-hexatriyne	9.50	9.48	8.5	7.93E-04
76	C_6H_4	benzyne	9.03	9.05	8.5	2.35E-04[d]
		3-hexene-1,5-diyne	9.07			
77	C_6H_5	phenyl radical	8.32	8.23	5.5	6.29E-05
78	C_6H_6	fulvene	8.36	8.41	6.0	3.19E-04
		benzene	9.24	9.24	7.5	3.46E-03
80	C_6H_8	1,3-cyclohexadiene	8.25	8.21	6.5	5.35E-04
82	C_6H_{10}	2,4-hexadiene	8.24	8.24	6.5	2.20E-04[d]
		4-methyl-1,3-pentadiene	8.26			
90	C_7H_6	5-ethenylidene-1,3-cyclopentadiene	8.29	8.29	8.0	4.32E-05
91	C_7H_7	benzyl radical	7.24	7.26	7.5	1.30E-04
92	C_7H_8	5-methylene-1,3-cyclohexadiene	7.90	7.91	7.0	6.05E-05
94	C_7H_{10}	3-methyl-3-isopropenyl-cyclopropene	7.84	7.87	6.0	3.12E-04
98	C_7H_{14}	cycloheptane	9.90	9.92	5.5	6.54E-04
102	C_8H_6	phenylacetylene	8.82	8.84	8.0	1.03E-03
104	C_8H_8	3,6-bis(methylene)-1,4-cyclohexadiene	7.87	7.86	7.5	2.69E-04
		styrene	8.46	8.49	6.0	1.51E-03
105	C_8H_9	2-methylbenzyl radical	7.07	7.09	7.5	2.51E-04
116	C_9H_8	indene	8.14	8.16	7.5	4.81E-04
118	C_9H_{10}	allylbenzene	7.80	7.74	6.0	1.69E-04
		β-methylstyrene	8.35	8.25	6.0	1.47E-03
120	C_8H_8O	dihydrobenzofuran	7.65	7.59		trace level
128	$C_{10}H_8$	naphthalene	8.14	8.16	7.5	4.66E-04
130	$C_{10}H_{10}$	3-methylindene	7.97	7.90	6.5	2.03E-04
132	$C_{10}H_{12}$	1,3-dimethyl-2-vinylbenzene	8.10	8.10	6.0	3.94E-04
134	$C_{10}H_{14}$	durene	8.06	8.04	3.5	2.46E-04
		prehnitene	8.16	8.22	3.5	1.61E-03
136	$C_{10}H_{16}$	trans,trans-1,6-cyclodecadiene	8.05	8.06	5.5	4.62E-05
140	$C_{10}H_{20}$	1-decene	9.42	9.41	3.5	7.58E-04
142	$C_{11}H_{10}$	1-methylnaphthalene	7.96	7.97	7.0	1.16E-04
144	$C_{11}H_{12}$	1,2,3,4-tetrahydro-1-methylene-naphthalene	7.90	7.81	7.0	6.82E-05
146	$C_{11}H_{14}$	cyclopentylbenzene	7.90	7.90	4.0	1.25E-04
148	$C_{11}H_{16}$	pentamethylbenzene	7.92	7.98	5.0	2.63E-04
152	$C_{12}H_8$	acenaphthylene	8.12	8.11	7.5	1.18E-04
154	$C_{12}H_{10}$	(*E*,*E*)-1-phenylhexa-1,3-dien-5-yne	7.90	7.93	5.0	4.48E-05
156	$C_{12}H_{12}$	1,4-dimethylnaphthalene	7.78	7.80	5.5	3.09E-05
166	$C_{13}H_{10}$	fluorene	7.91	7.85	8.0	5.59E-05
168	$C_{13}H_{12}$	2-methylbiphenyl	8.10	8.05	4.5	3.52E-05

Table 2 (Continued)

mass	formula	species	IE (eV) literature[a]	IE (eV) measured[b]	mole fraction peak position (mm)	mole fraction X_{MAX}
178	$C_{14}H_{10}$	phenanthrene	7.89	7.89	7.5	2.52E-05
190	$C_{15}H_{10}$	cyclopropa[*b*]anthracene	7.39	7.45	8.0	4.93E-06

[a] Refers to ref 38 except for specific description. [b] The experimental error for measured IEs in this work is ±0.05 eV for species with strong signals and ±0.10 eV for species with weak signals. [c] Refers to ref 50. [d] The value is the total maximum mole fraction of this mass; for example, the maximum mole fraction of 2.35×10^{-4} for mass 76 includes the contribution from both benzyne and 3-hexene-1,5-diyne. [e] Refers to ref 42.

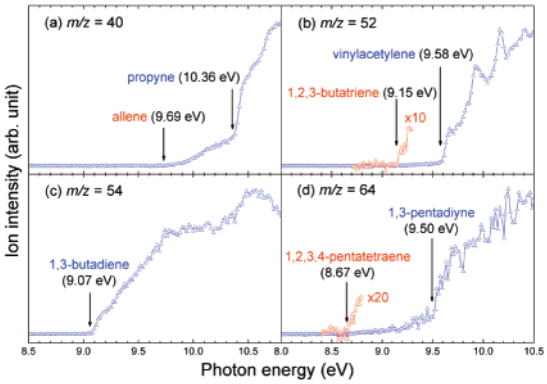

Figure 2. PIE spectra of some small hydrocarbon intermediates sampled from the rich gasoline flame: (a) $m/z = 40$; (b) $m/z = 52$; (c) $m/z = 54$; (d) $m/z = 64$. The recommended species are indicated above the corresponding thresholds, along with their literature IEs.

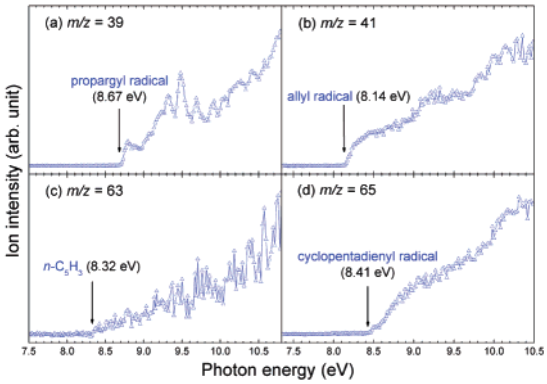

Figure 4. PIE spectra of some radicals sampled from the rich gasoline flame: (a) $m/z = 39$; (b) $m/z = 41$; (c) $m/z = 63$; (d) $m/z = 65$. The recommended species are indicated above the corresponding thresholds, along with their literature IEs.

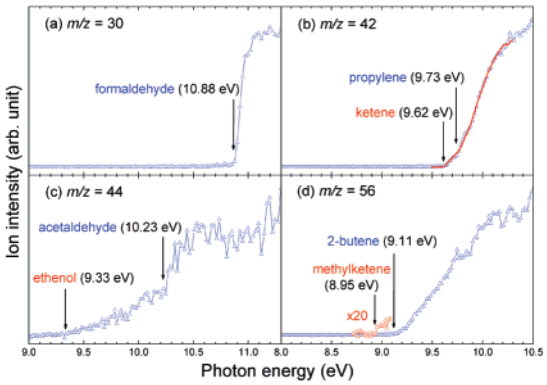

Figure 3. PIE spectra of some oxygenated intermediates sampled from the rich gasoline flame: (a) $m/z = 30$; (b) $m/z = 42$; (c) $m/z = 44$; (d) $m/z = 56$. The solid curve in Figure 3b shows the computed average photoionization cross section for a mixture of 34% ketene and 66% propylene. The recommended species are indicated above the corresponding thresholds, along with their literature IEs.

of 10 to clearly reveal the onset at 9.15 eV, which belongs to 1,2,3-butatriene (IE = 9.15 eV).[38] For $m/z = 54$, the only observed threshold at 9.07 eV is attributed to the ionization of 1,3-butadiene (IE = 9.07 eV),[38] which is identified as a hazardous air pollutant by the 1990 U.S. Clean Air Act having a cancer risk potency more than 25 times higher than that of benzene.[13] Figure 2d displays the PIE spectra of $m/z = 64$, which are partly amplified by a factor of 20. The photoionizations of 1,2,3,4-pentatetraene (IE = 8.67 eV)[38] and 1,3-pentadiyne (IE = 9.50 eV)[38] are responsible for the onsets at 8.65 and 9.50 eV, respectively. Besides the mentioned species, eight small hydrocarbon intermediates are also identified, including acetylene, ethylene, 1,3-butadiyne, 1,3-cyclopentadiene, and so forth.

Figure 3 shows four PIE spectra of oxygenated hydrocarbons sampled from the rich gasoline flame. The only threshold at 10.85 eV in Figure 3a indicates the existence of formaldehyde (IE = 10.88 eV),[38] which is one of the dominant oxygenated toxic substances associated with combustion processes.[2] In Figure 3b, the clear onset near 9.61 eV corresponds to the literature IE of ketene (9.62 eV).[38] As seen from the same figure, another onset around 9.72 eV can only be ambiguously observed, which is attributed to the photoionization of a hydrocarbon intermediate, propylene (IE = 9.73 eV).[38] To validate its presence, we calculated the relative photoionization cross sections for pure ketene and mixtures of ketene and propylene with different isomeric compositions. The computed cross section of each mixture is the respective weighted sum of the individual cross sections measured for ketene and propylene.[32,39] The result shows that the measured PIE spectra perfectly fit the scaled photoionization cross section for a mixture of 34% ketene and 66% propylene. Considering the uncertainty in curve fitting, an isomeric composition is determined to be of 34 ± 5% ketene and 66 ± 5% propylene in this flame. Figure 3c displays the PIE spectra of $m/z = 44$ with photon energies ranging from 9.00 to 11.30 eV. Two thresholds near 9.32 and 10.25 eV are measured from the spectra, corresponding to the literature IEs of ethenol (9.33 eV)[38] and acetaldehyde (10.23 eV).[38] The former is the smallest one of the enols, which are newly detected by Taatjes et al.,[40] while the latter is another important oxygenated toxic substance besides formaldehyde.[2] As shown in Figure 3d, an obvious threshold at 9.13 eV on the PIE spectra of $m/z = 56$ implies that 2-butene (IE = 9.11 eV)[38] is the dominant species. In addition, the amplified spectra from 8.72 to 9.08 eV by a factor of 20 show an onset near 8.94 eV, corresponding to the literature IE of methylketene (8.95 eV).[38] Compared with hydrocarbon intermediates, the amount of observed oxygenated intermediates is extremely low, as methanol and dihydrobenzofuran (C_8H_8O) are the only other ones in this flame. The low oxygen content in a fuel-rich flame can limit the formation of oxygenates, which should be the major reason.

(39) Vogt, J.; Williamson, A. D.; Beauchamp, J. L. *J. Am. Chem. Soc.* **1978**, *100*, 3478−3483.

(40) Taatjes, C. A.; Hansen, N.; McIlroy, A.; Miller, J. A.; Senosiain, J. P.; Klippenstein, S. J.; Qi, F.; Sheng, L. S.; Zhang, Y. W.; Cool, T. A.; Wang, J.; Westmoreland, P. R.; Law, M. E.; Kasper, T.; Kohse-Hoinghaus, K. *Science* **2005**, *308*, 1887−1889.

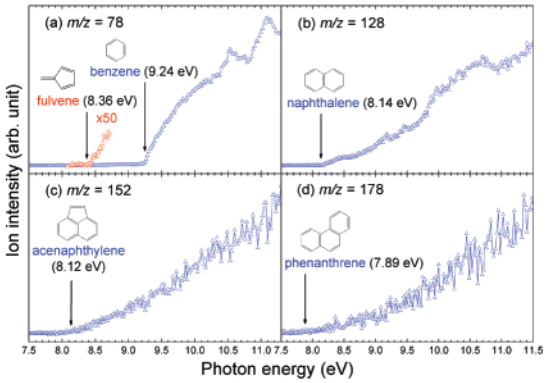

Figure 5. PIE spectra of some large hydrocarbon intermediates sampled from the rich gasoline flame: (a) $m/z = 78$; (b) $m/z = 128$; (c) $m/z = 152$; (d) $m/z = 178$. The recommended species are indicated above the corresponding thresholds, along with their literature IEs.

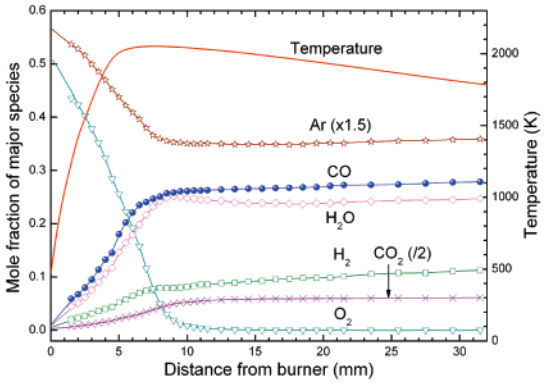

Figure 6. Mole fraction profiles of the major species (H_2, H_2O, CO, O_2, Ar, and CO_2) in the rich gasoline flame, along with the temperature profile.

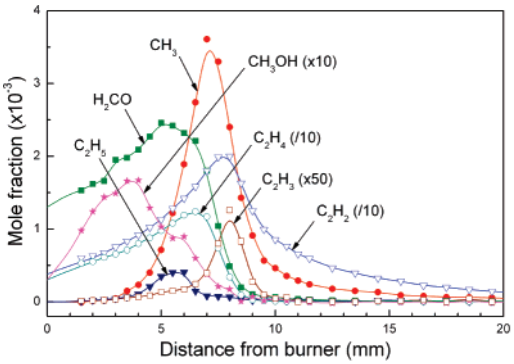

Figure 7. Mole fraction profiles of C_1 species and C_2 hydrocarbons in the rich gasoline flame.

Figure 4 shows four PIE spectra of radicals formed in this flame. The PIE spectra of $m/z = 39$ are presented in Figure 4a. The clear onset at 8.69 eV is attributed to the photoionization of the propargyl radical (IE = 8.67 eV),[38] which is the smallest π-conjugated species and has a series of autoionization Rydberg states corresponding to the peaks on the PIE spectra.[41] Figure 4b shows the PIE spectra of $m/z = 41$ with a single threshold at 8.14 eV. Thus, the existence of the allyl radical (IE = 8.14 eV)[38] can be confirmed in this flame. The PIE spectra of $m/z = 63$ are displayed in Figure 4c, which are recorded for a series of photon energies ranging from 7.50 to 10.80 eV. Only a threshold near 8.32 eV can be unambiguously measured, which is asserted to be the *n*-C_5H_3 radical (IE = 8.32 eV).[42] As seen from Figure 4d, the cyclopentadienyl radical with a literature IE of 8.41 eV[38] is responsible for the onset at 8.45 eV in the PIE spectra of $m/z = 65$. Besides the shown radicals, 12 other ones are listed in Table 2, that is, CH_3, C_2H_3, C_2H_5, C_3H_7, C_4H_3, C_4H_5 (three possible isomers), C_4H_7, C_6H_5, C_7H_7, and C_8H_9.

Figure 5 presents four PIE spectra of large hydrocarbon species, including three PAHs. This series contains 35 isomeric species. From Table 2, it can be concluded that most intermediates with a molecular weight greater than 78 are aromatics in this flame. The PIE spectra of $m/z = 78$ are shown in Figure 5a with photon energies ranging from 7.50 to 11.30 eV. From the spectra, we can find a clear threshold at 9.24 eV, indicating the presence of benzene (IE = 9.24 eV)[38] in this flame. However, the role of benzene in gasoline combustion can hardly be deduced from the measurement of PIE spectra because it is a component of gasoline. The region from 8.08 to 8.72 eV is amplified by a factor of 50 to exhibit the threshold near 8.41 eV. An isomer of benzene, which is called fulvene, with a literature IE of 8.36 eV,[38] is assigned to this threshold and has an evidently low concentration compared with that of benzene. Figure 5b shows the PIE spectra of $m/z = 128$ recorded for photon energies from 7.50 to 11.50 eV. The only onset at 8.16 eV implies the existence of naphthalene (IE = 8.14 eV).[38] In Figure 5c, a threshold of 8.11 eV can be measured on the PIE spectra of $m/z = 152$, which is attributed to the photoionization of another PAH species named acenaphthylene (IE = 8.12 eV).[38] For $m/z = 178$, two isomeric PAHs, that is, anthracene (IE = 7.44 eV)[38] and phenanthrene (IE = 7.89 eV),[38] can probably be formed in the rich gasoline flame, and these are found in hydrocarbon flames.[22] As seen from Figure 5d, we can observe a single threshold near 7.89 eV on the PIE spectra, which is in good agreement with the literature IE of phenanthrene. Thus, phenanthrene is identified as the only $C_{14}H_{10}$ species in this work, and the contribution from anthracene is negligible. The explanation of this phenomenon needs further modeling study.

3.3. Mole Fraction Profiles. Mole fraction profiles of most flame species are shown in Figures 6−11. As mentioned above, the maximum mole fractions of most species are listed in Table 2, including those gasoline components which have peak-shaped mole fraction profiles. Symbols in these figures represent the derived mole fractions of measured species, while B-spline curves are used to connect the symbols and extrapolate the profiles to 0 mm to guide the eye. To simplify the figures, mole fraction profiles of intermediates with the same or close molecular weights will not be displayed separately, and a total mole fraction profile of them will be shown instead. Mole fraction profiles of intermediates with IEs beyond the cutoff energy of the LiF window, for example, H, OH, and O radicals, are not presented in this study.

Figure 6 shows the mole fraction profiles of major flame species, including H_2, H_2O, CO, O_2, Ar, and CO_2. The gasoline components serving as fuels are almost exhausted around 7.5 mm. Thus, the region from 0 to 7.5 mm is recognized as the reaction zone where the oxidation of fuel is the major source for heat release, and the region farther than 7.5 mm can be defined as the post-flame zone. In general, mole fraction profiles of the gasoline components decrease monotonously as the distance from the burner surface increases, and thus they are not provided here. The concentration of O_2 decreases quickly to zero around 12.5 mm, indicating that O_2 is mostly consumed

(41) Zhang, T.; Tang, X. N.; Lau, K. C.; Ng, C. Y.; Nicolas, C.; Peterka, D. S.; Ahmed, M.; Morton, M. L.; Ruscic, B.; Yang, R.; Wei, L. X.; Huang, C. Q.; Yang, B.; Wang, J.; Sheng, L. S.; Zhang, Y. W.; Qi, F. *J. Chem. Phys.* **2006**, *124*, 074302.

(42) Yang, B.; Huang, C. Q.; Wei, L. X.; Wang, J.; Sheng, L. S.; Zhang, Y. W.; Qi, F.; Zheng, W. X.; Li, W. K. *Chem. Phys. Lett.* **2006**, *423*, 321−326.

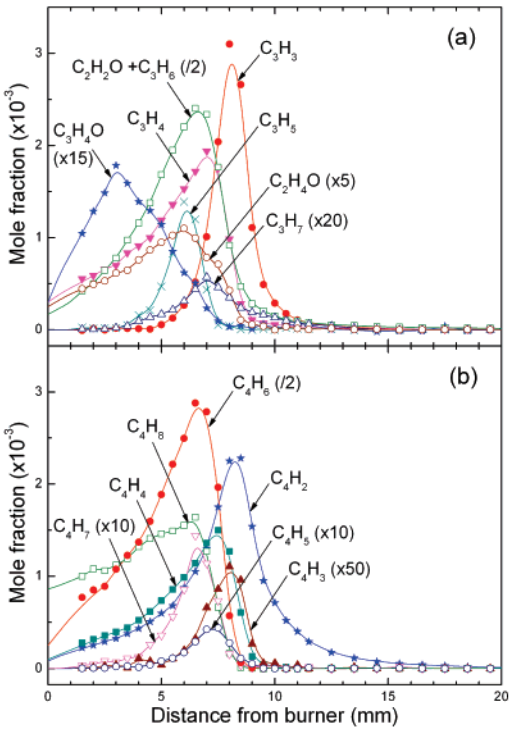

Figure 8. Mole fraction profiles of (a) C_2 oxygenated hydrocarbons and C_3 species and (b) C_4 species in the rich gasoline flame.

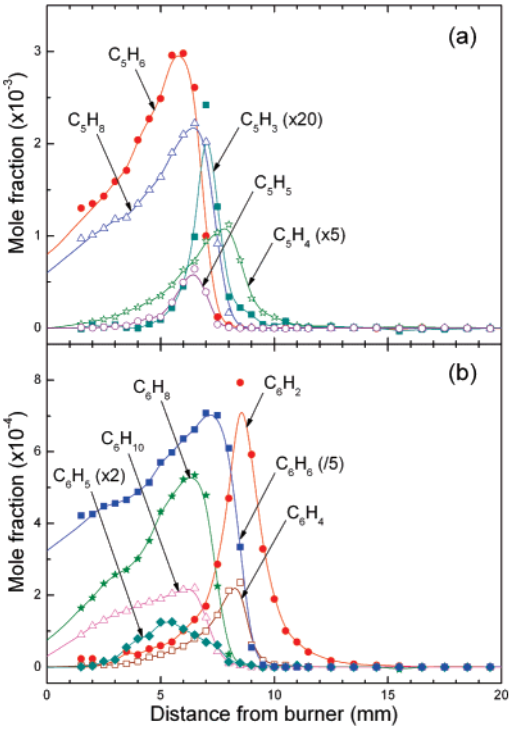

Figure 9. Mole fraction profiles of (a) C_5 species and (b) C_6 species in the rich gasoline flame.

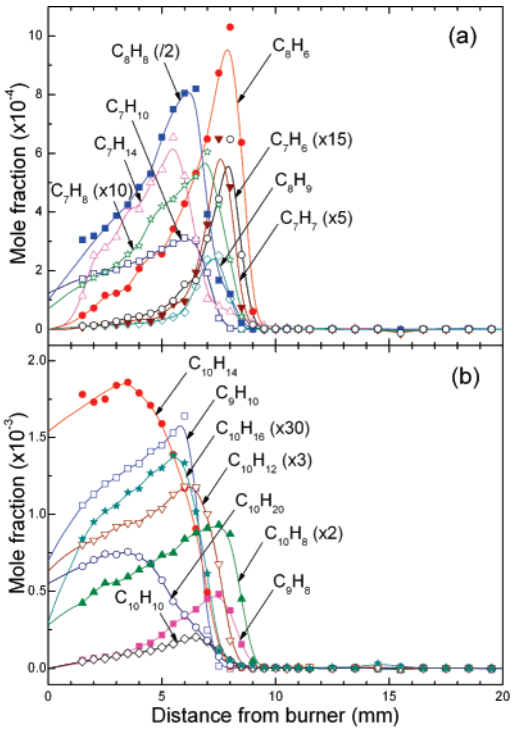

Figure 10. Mole fraction profiles of (a) C_7 and C_8 species and (b) C_9 and C_{10} species in the rich gasoline flame.

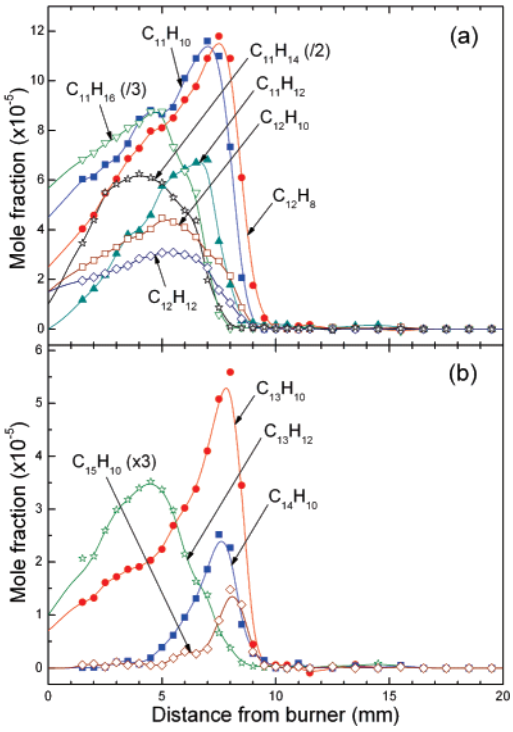

Figure 11. Mole fraction profiles of (a) C_{11} and C_{12} species and (b) C_{13} to C_{15} species in the rich gasoline flame.

before this position. H_2, H_2O, CO, and CO_2 are dominant products in rich hydrocarbon flames, with concentrations increasing sharply in the reaction zone. As seen from the figure, their mole fraction profiles continue to rise due to the oxidation of hydrocarbon intermediates and vary slowly after this position. The mole fractions of H_2, H_2O, CO, and CO_2 at 31.5 mm are 0.112, 0.247, 0.279, and 0.122, respectively. The mole fraction profile of Ar falls quickly from 0.387 in the reagent mixture to 0.233 around 10.0 mm and then climbs slowly to 0.239 in the post-flame zone. Besides, the calibrated temperature profile of this flame is also presented in this figure. The flame temperature has a sharp increase in the reaction zone to a maximum value of 2052 ± 100 K at 7.5 mm and then decreases gradually in the post-flame zone to 1783 ± 100 K at 31.5 mm.

The mole fraction profiles of C_1 species and C_2 hydrocarbons are displayed in Figure 7. Three C_1 species are detected in this flame, that is, the methyl radical, formaldehyde, and methanol. The methyl radical is one of the most common radicals in

hydrocarbon flames and a key chain carrier of many flame reactions. Its most possible source is the thermal cracking of methyl groups from gasoline components (especially those branched alkanes).[6] Here, its maximum mole fraction is measured to be 3.61×10^{-3} at 7.0 mm. As mentioned above, formaldehyde is identified in this work. It is the smallest oxygenated hydrocarbon and has a maximum mole fraction of 2.46×10^{-3} at 5.0 mm. Methanol is the other measured C_1 species, with a maximum mole fraction of 1.67×10^{-4} at 4.0 mm. Its major formation pathway is considered to be the recombination of methyl and hydroxyl radicals in previous studies.[43,44] Acetylene, the vinyl radical, ethylene, and the ethyl radical are identified as C_2 hydrocarbons in this work, and ethane is not detected in this flame, which is identical to the findings of previous studies.[22,30] Here, we measure the respective maximum mole fractions of ethyl and vinyl radicals to be 4.07×10^{-4} at 6.0 mm and 2.52×10^{-5} at 8.0 mm. Though not detected in this work, the formyl radical with $m/z = 29$, as well as ethane with $m/z = 30$, should also be taken into consideration for modeling purposes. As the smallest alkene and alkyne, ethylene and acetylene are the richest intermediates in this flame with the highest mole fractions of 1.24×10^{-2} and 2.00×10^{-2}, respectively. Warnatz concluded that these species have a chain formation sequence in small hydrocarbon flames, which starts from the self-combination of the methyl radical.[45] In brief, ethane, the ethyl radical, and ethylene are possible products of methyl recombination, and ethane can undergo a hydrogen abstraction to produce the ethyl radical, whose dominant destruction channel is the hydrogen abstraction to form ethylene; ethylene then reacts with some active radicals and produces the vinyl radical, which is the major precursor of acetylene.[45,46] In addition, the direct decomposition of gasoline components and other large intermediates may also play important roles for the formation of these C_2 hydrocarbons and other small hydrocarbons.

Figure 8a shows the mole fraction profiles of C_2 oxygenates and C_3 species. As mentioned above, two species of mass 42, that is, ketene and propylene, are identified in this flame. The strongest ion signal for $m/z = 42$ is measured at 6.5 mm where the composition is $34 \pm 5\%$ for ketene and $66 \pm 5\%$ for propylene. Thus, the mole fractions of ketene and propylene at this position are 2.45×10^{-3} and 4.76×10^{-3}, respectively. Both species are important in hydrocarbon combustion: ketene is responsible for the formation of formaldehyde, which initiates the classical C_1 oxidation pathway ($CH_2CO \rightarrow CH_2O \rightarrow HCO \rightarrow CO \rightarrow CO_2$),[43] and propylene can undergo a series of hydrogen abstractions and form smaller C_3 hydrocarbons. For $m/z = 44$, acetaldehyde and ethenol are distinguished with corresponding maximum mole fractions of 1.63×10^{-4} and 6.92×10^{-5}, both of which are common intermediates in hydrocarbon flames.[21−23,40] As the latest detected combustion intermediates, ethenol and larger enols are still mysterious because of their formation pathways and roles in hydrocarbon combustion. Taatjes and co-workers suggested that reactions of OH with alkenes should be a key source of enols in the preheat zone of low-pressure flames, and the addition of alkyl radicals to ethenol may provide one route to the larger enols.[40,47] They also presumed that tautomerization to produce acetaldehyde and the removal reaction to produce the vinyloxy radical may be possible consumption channels of ethenol. The isopropyl radical is the dominant species for $m/z = 43$ and has a maximum mole fraction of 2.86×10^{-5} at 7.0 mm and can react with O_2 to produce propylene.[48] As the only detected C_3H_5 species, the allyl radical is mainly produced via the hydrogen abstraction from propylene and the decomposition of larger hydrocarbons, and its profile reaches a peak value of 1.39×10^{-3} at 6.0 mm. The consecutive hydrogen abstraction from the allyl radical can lead to the formation of allene, whose tautomer is propyne, as discussed in the previous section. The maximum mole fractions of allene and propyne are 6.36×10^{-4} and 1.34×10^{-3}, respectively. The smallest C_3 hydrocarbon in this work is the propargyl radical, which plays an important role in hydrocarbon flames, chemical vapor deposition processes, and interstellar media. It can undergo a self-combination reaction and bimolecular reaction with the allyl radical to form benzene and the phenyl radical, and its formation is related to the hydrogen abstraction of allene and propyne as suggested by Law et al.[49] Here, we measure the peak value of its mole fraction profile to be 3.10×10^{-3} at 8.0 mm. Methylketene is the only observed C_3 oxygenated species with a maximum mole fraction of 1.19×10^{-4} at 3.0 mm, which can be formed from the oxidation of some C_3 and C_4 hydrocarbons such as propylene, 2-butene, and the 1-butyn-3-yl radical.[48]

The mole fraction profiles of C_4 species are shown in Figure 8b. There is a big family of C_4 hydrocarbons in this flame with two to eight hydrogen atoms in the molecule. As mentioned above, the hydrocarbon intermediate for $m/z = 56$ is identified to be 2-butene, which has a maximum mole fraction of 1.64×10^{-3} at 6.5 mm. Its hydrogen abstraction product is the 1-buten-3-yl radical (C_4H_7), with a maximum mole fraction of 1.44×10^{-4} at 6.5 mm. The species for $m/z = 54$ has been identified to be 1,3-butadiene by measurement of the PIE spectra. Three isomers, that is, but-2-yn-1-yl (CH_3CCCH_2), 1-butyn-3-yl (CH_3CHCCH), and *i*-C_4H_5 (CH_2CHCCH_2) radicals, contribute to the C_4H_5 profile. The detailed identification of these three C_4H_5 radicals in several flames, as well as the chemistry of *i*-C_4H_5, have been reported by Hansen et al.[50] However, the roles of but-2-yn-1-yl and 1-butyn-3-yl radicals in soot formation are still unknown and need further investigation. In this work, the peak mole fraction of *i*-C_4H_5 is measured to be 6.26×10^{-6}, while the other two radicals have a total maximum mole fraction of 3.75×10^{-5} at 7.5 mm. C_4H_4 consists of 1,2,3-butatriene and vinylacetylene with maximum mole fractions of 1.20×10^{-4} and 1.38×10^{-3}, respectively. Both of them can undergo a hydrogen abstraction to form the *i*-C_4H_3 (CH_2CCCH) radical. Hansen et al. did calculations of Franck−Condon factors and heats of formation for this radical.[50] On the basis of their work, we can confirm the existence of the *i*-C_4H_3 radical in this flame and measure its maximum mole fraction to be 2.21×10^{-5} at 8.0 mm. For C_4H_2, only one species, named diacetylene, is responsible, and its mole fraction profile has a peak value of 2.28×10^{-3} at 8.5 mm.

(43) Decottignies, V.; Gasnot, L.; Pauwels, J. F. *Combust. Flame* **2002**, *130*, 225−240.
(44) Zervas, E.; Poulopoulos, S.; Philippopoulos, C. *Fuel* **2006**, *85*, 333−339.
(45) Warnatz, J. *Proc. Combust. Inst.* **1981**, *18*, 369−384.
(46) Bhargava, A.; Westmoreland, P. R. *Combust. Flame* **1998**, *115*, 456−467.
(47) Taatjes, C. A.; Hansen, N.; Miller, J. A.; Cool, T. A.; Wang, J.; Westmoreland, P. R.; Law, M. E.; Kasper, T.; Kohse-Hoinghaus, K. *J. Phys. Chem. A* **2006**, *110*, 3254−3260.
(48) Marinov, N. M.; Pitz, W. J.; Westbrook, C. K.; Vincitore, A. M.; Castaldi, M. J.; Senkan, S. M. *Combust. Flame* **1998**, *114*, 192−213.
(49) Law, M. E.; Carriere, T.; Westmoreland, P. R. *Proc. Combust. Inst.* **2005**, *30*, 1353−1361.
(50) Hansen, N.; Klippenstein, S. J.; Taatjes, C. A.; Miller, J. A.; Wang, J.; Cool, T. A.; Yang, B.; Yang, R.; Huang, C. Q.; Wang, J.; Qi, F.; Law, M. E.; Westmoreland, P. R. *J. Phys. Chem. A* **2006**, *110*, 3670−3678.

Figure 9 displays the mole fraction profiles of C_5 and C_6 species, which are all oxygen-free. Among the species shown in Figure 9a, the largest one is C_5H_8, consisting of 1,3-pentadiene and 2-methyl-1,3-butadiene, and their maximum mole fractions are 1.58×10^{-3} and 6.33×10^{-4}, respectively. For $m/z = 66$, 1,3-cyclopentadiene is the only intermediate existing in this flame, and its profile has a peak value of 2.98×10^{-3} at 6.0 mm. It can be produced from the addition of acetylene to the allyl radical and destroyed via hydrogen abstraction to form the cyclopentadienyl radical. As shown in Figure 2d, 1,2,3,4-pentatetraene and 1,3-pentadiyne are both C_5H_4 species. The maximum mole fraction of 1,3-pentadiyne is 2.25×10^{-4} at 8.0 mm, while 1,2,3,4-pentatetraene has an extremely low concentration of "trace level" (less than 1 ppm). The corresponding species for $m/z = 63$ and 65 should be radicals with formulas of C_5H_3 and C_5H_5, which have many possible isomers in hydrocarbon flames. On the basis of the detailed identification presented by Yang et al.,[42] we detect the dominant C_5H_3 and C_5H_5 species to be HCCCHCCH and cyclopentadienyl radicals with maximum mole fractions of 1.21×10^{-4} and 6.42×10^{-4}, respectively.

The mole fraction profiles of intermediates containing six carbon atoms are shown in Figure 9b. Both 2,4-hexadiene and 4-methyl-1,3-pentadiene are considered as possible C_6H_{10} species since their IEs are close for clear identification. The total mole fraction profile is wide-shaped with a peak value of 2.20×10^{-4} at 6.5 mm. 1,3-Cyclohexadiene is detected to be the only species for $m/z = 80$, with a maximum mole fraction of 5.35×10^{-4} at 6.5 mm. For C_6H_6, the contributions from benzene and fulvene are evident. The maximum mole fractions are measured to be 3.46×10^{-3} for benzene and 3.19×10^{-4} for fulvene. Though benzene is a gasoline component, it is also considered as an intermediate in gasoline flames.[12] In this flame, the mole fraction profile of C_6H_6 has a high initial value near the burner surface and increases with the burner position before 7.5 mm, which is in agreement with the previous conclusion. A similar situation also occurs to other flame species which serve as both gasoline components and intermediates, for example, 1,3-cyclohexadiene, naphthalene, 1-decene, and so forth. The phenyl radical, an important chain carrier in the low-temperature oxidation and pyrolysis of benzene, is detected for $m/z = 77$ in this flame. It has a maximum mole fraction of 6.29×10^{-5} at 5.5 mm, which is the lowest among these C_6 species. From the measurement of PIE spectra for $m/z = 76$, two isomers of C_6H_4, that is, benzyne and 3-hexene-1,5-diyne, probably exist in this flame. The total mole fraction profile reaches a peak value of 2.35×10^{-4} at 8.5 mm. As shown in the figure, the smallest observed C_6 species is C_6H_2, with a narrow-shaped peak and maximum mole fraction of 7.93×10^{-4} at 8.5 mm. Its formation route may relate to the addition of acetylene to 1,3-butadiyne, as proposed by Yang et al.[22]

Figure 10a shows the mole fraction profiles of C_7 and C_8 species. Five C_7 hydrocarbons, as well as three C_8 hydrocarbons, are detected in this work. C_7H_6 is ascribed to 5-ethenylidene-1,3-cyclopentadiene, with a maximum mole fraction of 4.32×10^{-5} at 8.0 mm. C_7H_7 corresponds to the benzyl radical with a maximum mole fraction of 1.30×10^{-4} at 7.5 mm, which was also detected in the rich benzene flame.[22] For $m/z = 92$, two isomers of C_7H_8 are distinguished to be toluene and 5-methylene-1,3-cyclohexadiene. The former is a gasoline component and serves as fuel in this flame, while the latter is an intermediate with a maximum mole fraction of 6.05×10^{-5} at 7.0 mm. Thus, 5-methylene-1,3-cyclohexadiene is the only C_7H_8 species listed in Table 2. Two other C_7 hydrocarbons, C_7H_{10} and C_7H_{14}, are identified to be 3-methyl-3-isopropenyl-cyclopropene and cycloheptane, with maximum mole fractions of 3.12×10^{-4} and 6.54×10^{-4}, respectively. Phenylacetylene is the only C_8H_6 species, and its profile has a peak value of 1.03×10^{-3} at 8.0 mm. The species for $m/z = 104$ is assigned to two isomers of C_8H_8; one is 3,6-bis(methylene)-1,4-cyclohexadiene, with a peak mole fraction of 2.69×10^{-4} at 7.5 mm, and the other is styrene, with a peak value of 1.51×10^{-3} at 6.0 mm. A total maximum mole fraction of them is measured to be 1.64×10^{-3} at 6.5 mm. As the largest radical detected in this flame, the 2-methylbenzyl radical is the only C_8H_9 species with a maximum mole fraction of 2.51×10^{-4} at 7.5 mm. Besides these intermediates, a species with $m/z = 120$ is also detected in the present work. From the PIE spectra, only one threshold near 7.59 eV can be measured, which is very close to the literature IE of dihydrobenzofuran, and IEs of other stable species with this mass are all larger than 8 eV. Thus, the existence of dihydrobenzofuran in this flame can be confirmed. However, its concentration is too low to be measured, and a peak value of less than 1 ppm is evaluated.

Figure 10b displays the mole fraction profiles of C_9 to C_{10} species. C_9H_8 corresponds to indene, with a maximum mole fraction of 4.81×10^{-4} at 7.5 mm, which is also detected in other flames of large hydrocarbons.[21,22,51] C_9H_{10} is composed of two isomers, that is, allylbenzene and β-methylstyrene, with respective peak mole fractions of 1.69×10^{-4} and 1.47×10^{-3}. Besides these three hydrocarbons, no other C_9 intermediate can be observed in this investigation. Naphthalene is the most common C_{10} hydrocarbon with two benzenoid rings connected together. As discussed above, it is also a gasoline component and has a maximum mole fraction of 4.66×10^{-4} at 7.5 mm. 3-Methylindene and 1,3-dimethyl-2-vinylbenzene are identified to be $C_{10}H_{10}$ and $C_{10}H_{12}$ species with maximum mole fractions of 2.03×10^{-4} and 3.94×10^{-4}, respectively. $C_{10}H_{14}$ contains contributions from two isomers in this flame, that is, durene and prehnitene. The peak values of their mole fraction profiles are measured to be 2.46×10^{-4} for durene and 1.61×10^{-3} for prehnitene. *trans*,*trans*-1,6-Cyclodecadiene ($C_{10}H_{16}$) and 1-decene ($C_{10}H_{20}$) are other C_{10} hydrocarbons with corresponding mole fractions of 4.62×10^{-5} at 5.5 mm and 7.58×10^{-4} at 3.5 mm.

Figure 11 shows the mole fraction profiles of C_{11} to C_{15} species. As seen from Figure 11a, four C_{11} hydrocarbons are identified in this flame, including 1-methylnaphthalene ($C_{11}H_{10}$), 1,2,3,4-tetrahydro-1-methylene-naphthalene ($C_{11}H_{12}$), cyclopentylbenzene ($C_{11}H_{14}$), and pentamethylbenzene ($C_{11}H_{16}$), with maximum mole fractions of 1.16×10^{-4}, 6.82×10^{-5}, 1.25×10^{-4}, and 2.63×10^{-4}, respectively. Figure 11a also shows the profiles of three C_{12} hydrocarbons, that is, acenaphthylene ($C_{12}H_8$), (*E*,*E*)-1-phenylhexa-1,3-dien-5-yne ($C_{12}H_{10}$), and 1,4-dimethylnaphthalene ($C_{12}H_{12}$), with corresponding peak values of 1.18×10^{-4}, 4.48×10^{-5}, and 3.09×10^{-5}. Figure 11b includes four species containing more than 13 carbon atoms. Fluorene and 2-methylbiphenyl are responsible for $C_{13}H_{10}$ and $C_{13}H_{12}$, and their maximum mole fractions are 5.59×10^{-5} at 8.0 mm and 3.52×10^{-5} at 4.5 mm, respectively. $C_{14}H_{10}$ is ascribed to phenanthrene with a maximum mole fraction of 2.52×10^{-5} at 7.5 mm. The largest species observed in the present work is cyclopropa[*b*]anthracene for $C_{15}H_{10}$, whose profile has a peak value of 4.93×10^{-6} at 8.0 mm.

(51) Defoeux, F.; Dias, V.; Renard, C.; Van Tiggelen, P. J.; Vandooren, J. *Proc. Combust. Inst.* **2005**, *30*, 1407−1415.

4. Discussion

4.1. Comparison between the Lean and Rich Gasoline Flames. The comparison between the lean gasoline flame investigated by Huang et al.[21] and this flame reveals the variations of combustion processes induced by different fuel/O_2 ratios. The lean gasoline flame has a lot of oxygenated intermediates from C_1 to C_{12}, while only seven are detected in the rich flame. On the contrary, the rich gasoline flame contains a large amount of hydrocarbons compared with the lean flame. For those detected in both flames, the differences between the mole fractions are obvious: most hydrocarbon intermediates have higher concentrations in the rich flame than in the lean flame, which is opposite of the situation of most oxygenated species. In addition, the temperature of the lean gasoline flame is higher than that of the rich flame. All of these differences can be interpreted as follows. Compared with the lean flame, the low oxygen content in this flame can limit the oxidation processes and reduce the heat release, which ultimately decreases the flame temperature, the amount of oxygenated intermediates, and their concentrations. On the other hand, recombination processes play a more important role in the destruction of radicals than that of oxidation processes; thus, the amount of hydrocarbon intermediates and their concentrations in the rich gasoline flame become much higher than those in the lean flame.

4.2. Possible Formation Pathways of Toxics and PAHs. For the consideration of environmental security and human health, the toxic emissions from gasoline-fueled engines should be controlled at a low level. A lot of previous investigations have presumed the possible formation routes of toxic substances and PAHs associated with gasoline combustion.[6,12,52] Since gasoline combustion in real engines is a complex system, the researchers paid most of their attention to the emissions produced via incomplete combustion, which is divided into two groups, that is, unburnt fuels and partial oxidation products. Their works proposed relationships between gasoline components and exhaust emissions, which is valuable for understanding combustion processes of gasoline and controlling toxic emission levels. However, the roles of intermediates (especially radicals) in the formation of emissions are still insufficiently studied due to the limitations of measurement techniques. Here, we will focus on the formation mechanism of toxic substances and PAHs from small combustion intermediates.

A lot of hazardous hydrocarbons and oxygenates are formed in this flame, including aldehydes, methanol, 1,3-butadiene, and some aromatics. As discussed above, methanol is mainly produced from the recombination of methyl and hydroxyl radicals in hydrocarbon flames. This route should also be the dominant one for methanol formation in this flame, because the gasoline contains no oxygenated component, which is concluded to be the major source of methanol in the combustion of blended gasoline.[12] Formaldehyde is dominantly produced from the oxidation of methyl radicals and ketene;[43,45] meanwhile, the decomposition of some oxygenates, such as methanol and acetaldehyde, is also important for its formation.[12,53] As the other aldehyde derivative detected in this flame, acetaldehyde can be formed via the tautomerization of ethenol and the recombination of methyl and formyl radicals.[43,47] For 1,3-butadiene, the decompositions of some gasoline components, that is, 1-pentene, 1-hexene, and cyclohexane, are considered to have significant contributions by previous works.[6] However, the investigated gasoline does not contain these species, indicating that the roles of small intermediates and other large hydrocarbons are important for the formation of 1,3-butadiene. In this work, a remarkable concentration is measured for the 1-buten-3-yl radical, which can undergo a hydrogen abstraction and then produce 1,3-butadiene. The maximum mole fractions of 1,3-butadiene and the 1-buten-3-yl radical are about 4 and 5 times greater than those in the rich benzene flame[22] and 110 and 70 times greater than those in the rich ethylene flame,[54] which shows a strong relationship between 1,3-butadiene and the 1-buten-3-yl radical. In addition, the reaction of the vinyl radical and ethylene to produce 1,3-butadiene should also be taken into account.[48]

Numerous aromatics are observed with high concentrations in this flame. A partial reason is that the gasoline contains a mass of aromatic components, such as benzene, toluene, ethylbenzene, xylenes, naphthalene, and so forth. In aliphatic hydrocarbon flames, generation processes of the first and second benzenoid ring are thought to be key steps for the formation of other aromatics and PAHs.[55−57] The dominant source of benzene in these flames is from the bimolecular reactions of some precursors, for example, self-combination of the propargyl radical and the recombination of propargyl and allyl radicals; i-C_4H_3 and vinyl radicals; the i-C_4H_5 radical; acetylene, cyclopentadienyl, and methyl radicals, and so forth.[56,58,59] However, the major source of benzene production is suggested to be the dealkylation of toluene and xylenes in previous gasoline flames.[6] In this flame, benzene has an extremely higher maximum mole fraction than other hydrocarbon flames, and the difference is much greater than those of its precursors. For example, we compared the concentrations of benzene and its most important precursor, the propargyl radical, in this flame with those in the rich ethylene and propane flames.[30,54] The maximum mole fraction of benzene in this flame is about 100 and 230 times higher than those in the ethylene and propane flames, while the maximum mole fraction of the propargyl radical increased by about 6 and 50 times, respectively. It is obvious that the concentration of benzene is not very sensitive to that of the propargyl radical. The same situation also occurs with other benzene precursors. Thus, it can be concluded that the decomposition of higher aromatics is much more important for benzene formation than the recombination of small intermediates in this flame.

Naphthalene is one of the most ordinary PAHs and also the smallest one. As the rate-controlling steps for the formation of PAHs and soot particles, its generation is more important than that of benzene in aromatic hydrocarbon flames.[56] From the identification of gasoline components, few alkylnaphthalenes are measured with low concentrations compared with those of alkylbenzenes,[1] which implies that naphthalene is less likely to be produced from the decomposition of larger aromatics in gasoline flames. Hence, the roles of intermediate reactions, for example, the addition of the propargyl radical to the benzyl radical and the combination of two cyclopentadienyl radicals[56] should be more important. Since the comprehensive studies of

(52) Zervas, E.; Montagne, X.; Lahaye, J. *J. Air Waste Manage. Assoc.* **1999**, *49*, 1304−1314.
(53) McEnally, C. S.; Pfefferle, L. D. *Proc. Combust. Inst.* **2005**, *30*, 1363−1370.
(54) Bhargava, A.; Westmoreland, P. R. *Combust. Flame* **1998**, *113*, 333−347.
(55) Frenklach, M.; Clary, D. W.; Gardiner, J. W. C.; Stein, S. E. *Proc. Combust. Inst.* **1984**, *20*, 887−901.
(56) McEnally, C. S.; Pfefferle, L. D.; Atakan, B.; Kohse-Hoinghaus, K. *Prog. Energy Combust. Sci.* **2006**, *32*, 247−294.
(57) Glassman, I. *Proc. Combust. Inst.* **1988**, *22*, 295−311.
(58) Miller, J. A.; Melius, C. F. *Combust. Flame* **1992**, *91*, 21−39.
(59) Richter, H.; Howard, J. B. *Phys. Chem. Chem. Phys.* **2002**, *4*, 2038−2055.

large hydrocarbon flames are limited, we only compared the concentrations of naphthalene and its precursors between this flame and the rich benzene flame. The maximum mole fractions of naphthalene, the propargyl radical, the cyclopentadienyl radical, and the benzyl radical in this flame are all about twice of those in the benzene flame, indicating that the concentration of naphthalene increases directly with those of its precursors. Thus, the formation of naphthalene in the rich gasoline flame is greatly related to the intermediate reactions, which is identical to the situation in the rich benzene flame. In addition, other aromatics and PAHs can be formed by the growth of additional benzenoid rings to the initial structure,[56] which need more experimental and theoretical studies in the future.

5. Conclusion

A rich premixed gasoline/O_2/Ar flame at a low pressure with an equivalence ratio (ϕ) of 1.73 has been investigated using the tunable synchrotron photoionization and molecular-beam mass spectrometry techniques. Flame species, including isomeric intermediates, are unambiguously identified with measurements of photoionization efficiency spectra by scanning the photon energy. Mole fraction profiles of most observed species are derived from the results of scanning the burner position at selected photon energies near ionization thresholds, and the flame temperature profile is recorded using a Pt/Pt-13%Rh thermocouple. The possible formation pathways of some flame species, that is, key intermediates, toxic substances, and PAHs, have been discussed, along with the comparison between the lean and rich conditions. On the basis of previous works, we can conclude that the role of intermediate recombination in the formation of toxic substances and PAHs is as significant as that of the direct decomposition of gasoline components. For example, the formation of benzene is mostly associated with the dealkylation of toluene and xylenes, while the formation of naphthalene is considered as the result of the recombination of radicals. The comprehensive experimental data will be helpful for understanding the combustion mechanism of gasoline and controlling the exhaust emission levels from gasoline-fueled engines.

Acknowledgment. We thank the reviewers for constructive suggestions. The authors wish to thank the Chinese Academy of Sciences (CAS), Natural Science Foundation of China, for the funding support under grant nos. 20473081 and 20533040, and SRF for ROCS and SEM.

EF0700578